Original Article
Bulletin of Pure and Applied Sciences.
Chemistry , Vol.44 C, No.2
July-December 2025: P.78-90

http://www.bpasjournals.com/chemistry
Print version ISSN 0970 4620
Online version ISSN 2320 320X

Electrochemical Investigations of Al-8088/TiO2/SiC Hybrid Composites developed using stir Casting method

[1]Pruthviraj R.D.*, [2]Bhagyalakshmi H., [3]Santhosh Kumar A.S. and [4] Ramesha S.

Author's Affiliations:
[1,4]Department of chemistry, Rajarajeswari college of Engineering, VTU, Bangalore, Karnataka 560074, India.
[2]Department of chemistry, Dr. Ambedkar Institute of Technology, VTU, Bangalore, Karnataka 560056, India
[3]Department of Chemistry, Bangalore University, Jnanabharathi campus, Bangalore, Karnataka 560056, India

***Corresponding Author: Pruthviraj R.D.,** Department of chemistry, Rajarajeswari college of Engineering, VTU, Bangalore, Karnataka 560074, India.
E-mail: pruthvirajrd@gmail.com

ABSTRACT

Aluminium alloys are employed in aerospace, automotive, and other structural uses due to their high strength and lightweight qualities. Moreover, when aluminum alloys are exposed to different conditions at different temperatures, corrosion becomes a life-limiting problem. In this study Alumina (TiO2) and palm kernel shell ash (SiC) were used as reinforcement particles in Al 8088 matrix alloy, this work examines the corrosion behaviour of hybrid composites at various mix ratios. The method of double stir casting was employed to develop the composites. Both gravimetric analysis and electrochemical measurements were used to examine the corrosion behaviours of the composites in NaCl solutions. The results obtained by the gravimetric analysis, suggested that the composite film was defective and that corrosion products were forming on the specimens' surface. Pitting and general corrosion were the mechanisms of corrosion that were detected in the samples. The Al8088 matrix's reinforcements served as active locations for the onset of corrosion. E Corr and I corr in 3.5% NaCl varied from −220.62 to −899.46 mV and 5.45 to 40.87 µA/cm2, respectively, at 24 hours. At 72 hours, E Corr values were between 255.88 and −887.28 mV, while I corr values were between 7.19 and 16.85 µA/cm2. The samples under investigation's electrochemical corrosion behaviour were shown by the Nyquist and Bode plots, which connected the main surface responses to processes related to charge transfer. The samples' relative resistance to corrosion is determined by the thin oxide layer that develops on their surface.

Keywords: Hybrid Composites, NaCl, TiO2, SiC, Electrochemical studies, SEM.

Received on 02.03.2025, Revised on 05.05.2025, Accepted on 02.07.2025

How to cite this article: Pruthviraj R.D., Bhagyalakshmi H., Santhosh Kumar A.S. and Ramesha S. (2025). Electrochemical Investigations of Al-8088/TiO2/SiC Hybrid Composites developed using stir Casting method. *Bulletin of Pure and Applied Sciences-Chemistry,* 44C (2), 78-90.

INTRODUCTION

Numerous scientific research discoveries have contributed to the ongoing advancement of innovative engineering materials utilized in the automotive, marine, aviation, and building construction industries [1, 2, 3, 4]. Matrix classification is used to classify composite materials, which constitute a significant portion of sophisticated engineering materials [5, 6, 7]. One class of composite materials that is comparable to advanced engineering materials is metal matrix composite (MMC). As base matrices, several metal matrices, including Al, Mg, and Ti, have been used. On the other hand, most research has been done on an aluminium matrix composite (AMCs) due its mechanical properties [2, 8, 9]. AMCs, or aluminum matrix composites, are versatile materials used in mechanical engineering applications.

AMCs have been the subject of a lot of recent efforts due to their high specific strength and low thickness, good weight-to-strength ratio, good quality, and comparatively high wear resistance [9, 10, 11]. Excellent physical, thermal and mechanical qualities have been linked to the implementation of AMCs in automobiles and aircraft industries [9, 12]. To create AMCs, many monolithic and hybrid reinforcements have been added to aluminum matrices [1, 12, 13, 14]. In order to create the reinforcements, two different methods are used: either synthetic reinforcements (TiO2, TiO2, B_4C, and TiC) [15, 16] or combinations of two synthetic reinforcements or reinforcements made from utilizing agro-residue (RHA, BPA, CCA, SBA, and rice husk ash) [11, 12, 17].

In order to develop HCs, a variety of metallurgical techniques are accessible, such as squeeze casting, spray deposition, stir casting, high-energy ball milling, and powder metallurgy [18, 19]. Nonetheless, the stir casting process is mostly used because of its ease of use, affordability, and reasonably even dispersion of reinforcement particles throughout the matrix [2, 9, 18, 20, 21]. Reinforcement can improve the physico mechanical properties of HCs, but it can also drastically change their corrosion characteristics.

One crucial consideration when figuring out the potential uses for AMCs is to look at their corrosion behaviors [1]. The physico mechanical and tribological characteristics of hybrid reinforced HCs have been extensively studied; however, more research is required to comprehend the corrosion behavior of these materials, especially when partial or complete reinforcing with agro-residue ashes is involved. Pits are started by reinforcements in HCs, particularly at the secondary particles of the matrix. The aforementioned phenomenon may be ascribed to several chemical, electrochemical, or physical interactions among the matrix, reinforcements, and the corrosive environment under simulation [1].

Nanjan and Murali [9] examined the effects of reinforcing Al6061 with graphite, TiO2, and B4C at 4% and 5% using the stir casting method. After being immersed in solutions containing 1.M HCl and 3.5% NaCl, the produced samples were assessed. The outcomes demonstrated that there was good corrosion resistance in addition to strong mechanical properties. Under various aging scenarios, the effects of similar amounts (1-4 weight percent) of hybrid RHA and TiO2 particulates added to A356 alloy were examined. The samples created using the stir casting technique were immersed in solutions that contained 5% NaCl and 0.1 normal HCl. It was discovered that the composite's resistance to corrosion had improved [22].

In a setting containing 3.5 weight percent NaCl, Zakaria [1] examined the corrosion behavior of aluminum metal composites (AMCs) made of Al powder and TiO2 at both room temperature and high temperatures. We looked into how the size and volume percentage of TiO2 reinforcement affected the microstructure and corrosion behavior of the HCs that were produced. The corrosion resistance of Al/TiO2 HCs was higher than that of pure Al matrix.

The decrease in Al/TiO2 corrosion rate was caused by TiO2 particles being smaller and their volume % rising. An electrochemical analysis of composites consisting of fly ash, carbonized eggshell, and Al-SiC as a matrix in 3.5 weight

percent NaCl (2022) was carried out by Ononiwu et al. [23]. The analysis found that as the weight percentage of the reinforcement

When creating AMCs, the wood particle was utilized as reinforcement in the Al matrix, and the corrosion characteristics were examined. In comparison to the reinforced aluminium alloy, the study found that the unreinforced samples' corrosion resistance increased in a 3.5 weight percent NaCl solution [24]. Haridass et al. [6] examined the corrosion behaviour of AMCs made using hybrid reinforcement of TiO2 and rice husk ash (RHA) with Al8088 as the matrix. The AMCs were made by stir casting, and $AlCl_3$ was utilized as the corrosion solution. According to the study, when TiO2 and RHA addition rose, so did the hybrid reinforced AMCs' resistance to corrosion. Furthermore, compared to pure Al8088, the hybrid aluminium composites showed better corrosion resistance.

Due of the varied matrices, reinforcements, and production methods used, the corrosion behaviour of different AMCs has produced inconsistent results. Therefore, depending on the specified circumstances, there is no continuous trend of scientific discoveries. There are few studies in the literature on the corrosion characteristics of AMCs made with TiO2 and palm kernel shell ash (SiC). The impact of SiC and TiO2 particles on the corrosion susceptibility of Al8088/TiO2/SiC composites is not well understood. Thus, in this work, the corrosion susceptibility of artificially manufactured AMCs in a 3.5 weight percent NaCl solution was examined. Potentio dynamic polarization was investigated, and the weight loss of the composites in both solutions was calculated.

MATERIALS AND METHODS

Materials and Composite Production

The chemical composition of the Al8088 alloy was 0.48% magnesium, 0.43% silicon, 0.17% iron, 0.04% manganese with the rest being aluminium, while that of the SiC was 66.9% SiO_2, 6.46% TiO2, 5.72% Fe_2O_3, 5.52% CaO, 5.20% K_2O, 3.78% P_2O_5, 3.14% MgO, 0.53% TiO_2, and 2.75% loss on ignition. The TiO2 and SiC reinforcements have average particle sizes of around 30 and 40 μm, respectively. The designation of the composites created is shown in **Table 1**.

Table 1: Properties of Al8088

Name	Specification
Magnesium	2.2%-2.8% by wt
Chromium	0.15% -0.35% (maximum)
Copper	0.1% (maximum)
Iron	0.4% (maximum)
Manganese	0.1% (maximum)
Silicon	0.25% maximum
Zinc	0.1% (maximum)
Al	96.7%-95.9%

In accordance with numerous publications, the two-stir casting method was utilized as the production technique [5, 13, 25]. This technique is a liquid metallurgy route. The SIC and TiO2 particulates required per composition in the matrix alloy were evaluated via the charge calculation method. Inherent moisture removal as well as improving wettability of the reinforcement in the matrix was performed by preheating at 250°C. The matrix ingots were

charged and melted in a gas-fired crucible at a temperature above the liquidus temperature of the matrix alloy (750°C). This was done to guarantee that the matrix alloy melted completely. After charging the heated reinforcement particles into a semi-solid molten matrix alloy, the slurry was manually agitated for a duration of five to ten minutes. After that, the slurry was heated to 800°C and given another mechanical stir for ten minutes at 400 rpm. The slurry was finally poured into a sand mould that had been prepared and left to solidify. After solidification, the composite product was then obtained.

Preparation of Specimen

A sample of Ø30 × 3 mm was cut from each composition in Table 2. Every sample was ground between 240 and 1000 grits of TiO2 paper, cleaned with acetone, rinsed with water, and allowed to dry. A vernier gauge was used to determine the sample's thickness, and a digital electronic balance was used to measure the sample's weight. The samples' microstructures were investigated with a scanning electron microscope, Vega 3 TESCAN model.

Physical and Mechanical Properties

The physical characteristics of the composites, namely their density and porosity, were ascertained in accordance with the report by Prasad et al. [26]. Nonetheless, the ASTM E10-18 standard was used to calculate the composites' Brinell hardness value [27]. For the purpose of ensuring data reliability, the average hardness value of the four indents made on each sample was employed. In accordance with the ASTME8/E8M-16 standard, a 5 mm diameter sample and a 30 mm gauge length were used for the tensile test [28]. A strain rate of 10−3/s was employed with a universal testing machine (UTM) (Model No.: Instron 3369). To ensure the accuracy of the data, the curation process

Corrosion Test

Immersion Test/Gravimetric Measurement

Using a digital scale with 0.1 mg accuracy, weight loss was recorded to assess the corrosion rate of the hybrid Al composites. The corrosive environment was created as a 3.5 wt.% NaCl solution. Prior to being submerged into the two solutions individually, each specimen was weighed. Before reweighing, the samples were taken out of the solutions, cleaned, and dried (W_A). This process was run at room temperature for fifteen days.

The corrosion rates given in millimetre penetration per year (mm/year) and the weight loss rates were calculated. Photographs were used to inspect the deteriorated surfaces. A glass cover was placed on top of the jar for the samples in the elevated temperature corrosion test to stop evaporation. Using Equation (1) based on ASTM G31-12a [29], the weight loss measured was calculated and, using Equation (2), the corrosion rate was assessed.

Weight loss, $W = W^B - W^A$ Weight loss (1)

$$\text{CPR} = \frac{K \times W}{D \times A \times T}$$ Corrosion rate (2)

where CPR is the corrosion rate (mm/year), K is a constant (8.766×10^4), T is the time of exposure (h), A is the area (cm^2), W is the weight loss (mg), and D is the density of the material (g/cm^3).

Electrochemical Corrosion Test

The manufactured composite was subjected to accelerated electrochemical investigations utilizing the potentio dynamic technique. The 3.5 wt.% NaCl solution at 25 °C was used for the potentio dynamic measurements. Prior to putting the samples in the measuring vessel, they were polished and cleaned to a surface area of 1 cm^2. The composite sample served as the working electrode, while platinum acted as the electrode counter and silver/silver chloride (Ag/AgCl) serves as the reference electrode. To reach the requisite corrosion potential (E_{corr}) for the experiment, the apparatus was set for around 30 min to record the anodic polarization curves, an automated potential shift was applied at a rate of 10−3 V. The polarization measurements were carried out from -1.5 to +1.5 V at a scan rate of 0.0016 V/s in compliance with ASTM G102-89 [30]. The measurements were taken 24 and 72 hours after the different specimens were immersed in a 3.5 percent by weight NaCl solution. The Tafel plots of log current versus potential were used to calculate the corrosion potential (E corr) and corrosion

current densities (Icorr) for each sample. The potentiodynamic apparatus was used to obtain the electrochemical impedance spectrometry (EIS) measurement, which was then used to obtain the Nyquist and Bode plots.

RESULTS AND DISCUSSION

Microstructure of Produced Composite

The microstructure of the unreinforced matrix metal is shown in Figure 1a. The microstructure shows no signs of intermetallic grain. Figure 1b–e shows the microstructures of a few more exemplary samples. Figures 1b and 1d, respectively, show the microstructures of the monolithic reinforced samples of Al_2O_3 and MoS2. Nonetheless, Figure 1c, e displays the microstructures of the typical samples for the hybrid reinforced composites. The homogeneous distribution of reinforcement particles inside the matrix is evident. The composites that were created showed no signs of fracture development or increased pores Because of the chosen processing methods and parameters utilized in the composite synthesis, there is a sign of favourable wetting conditions between the reinforcing particles and the matrix [31, 32]. The micrographs displaying the evenly dispersed reinforcement particles validate the effectiveness of the twofold stir casting procedure in releasing the surface tension between the matrix alloy and the reinforcement particulates in the composite [5]. Consequently, during the double stir casting procedures, trapped air bubbles in the slurry are let to escape.

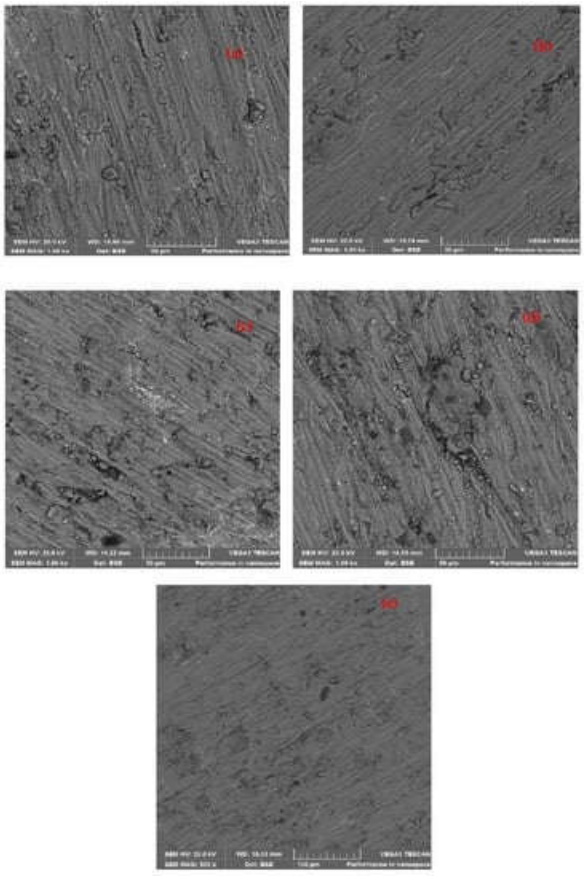

Figure 1: Scanning electron micrographs of (**a**) sample A0, (**b**) sample A1, (**c**) sample A5, (**d**) sample A6, (**e**) sample A9.

Physical and Mechanical Properties

The unreinforced alloy has a theoretical density of 2.7 g/cm3 and a percentage porosity of 2.063%. Sample A1 had the highest density (2.71 g/cm3), while sample A5 had the lowest density (2.56 g/cm3). Sample A6 came in second with 2.66 g/cm3. The amount of SIC particles in the matrix was the cause of the low density shown in samples A5 and A6SiC has a lower density than matrix alloy and TiO2. As a result, its presence lowers the composite's total density. However, because the density of TiO2 was higher than the matrix, sample A1's density was higher than sample A0's. The density of sample A9 was higher due to the higher concentration of TiO2 particles (8%) compared to SiC particles (2%) in the sample. It is well known that the majority of biomass reinforcement particles have lower densities, which inevitably affects the composite's total density [5]. The percentage porosity of all the samples is smaller than 2.4%, indicating that the composites that are formed are within the acceptable range for cast HCs [32]. The surface tension breakup between the matrix and the reinforcement particles was efficiently ensured by the processing way, which was reaffirmed by the acquired porosity percentage values. The strength, toughness, and wear resistance of any material are significantly influenced by its hardness value. Table 3 shows that the YS, the UTS, and Brinell's hardness value all followed a comparable trend. The unreinforced material (sample A0) has a YS of 78.84 MPa, a UTS of 116.09 MPa, and a hardness value of 73.02 BHN. The hardness value, YS, and UTS of Sample A1, reinforced with 2% TiO2, are 75.79 BHN, 84.47 MPa, and 124.47 MPa, respectively. The fact that TiO2 has a harder surface than the matrix alloy made this possible. Although the tiny amount of SiC (2%) in monolithic reinforced sample A6 produced a harder ness value achieved compared to sample A1, but greater than sample A0, SiC particles comprise hard phases of silica and other strengtheners. Much higher hardness values were obtained when TiO2 and SiC reinforcing particles were combined. A9, the sample with the highest hardness rating, contained 8% TiO2 and 2% SiC. Certain intermetallic can be added to the composites to increase their hardness. A high dislocation density or a rise in the volume of precipitated phases indicate an increase in hardness. Therefore, when the surface area of the additional reinforcing particles grows, so does the matrix grain size [33, 34].

The hardness of silica and other strengthening oxides in the SiC particles in the samples (A5, A6, and A9) led to enhanced YS and UTS compared to the unreinforced matrix, as the YS and UTS findings followed the sample pattern with the hardness value. However, because TiO2 is stronger than SiC, sample A1 of the monolithic reinforced samples A1 and A6 with 2% TiO2 and 2% SiC, respectively, showed greater YS and UTS. There are three involved processes for the YS and UTS improvement in HCS: the mismatch between the matrix and reinforcement's coefficient of thermal expansion (CTE), the Orowan strengthening mechanisms, and the grain boundary strengthening known as the Hall–Petch effect [35]. The samples generated were found to have an elongation percentage ranging from 5.0% to 7.6%. Sample A0, the unreinforced alloy, had the best percentage of elongation. Sample A9 exhibits the lowest percentage of elongation (5.0%), which may be ascribed to its capacity to sustain plastic strain due to the hard components found in the SiC and TiO2 particles. As a result, It was observed that the matrix's ductile phase and the composite's percentage elongation had decreased [10, 21].

Gravimetric Analysis

Corrosion Behaviour in 3.5 wt.% NaCl Environment

The weight changes and corrosion rates of the samples in a 3.5% salt solution are shown against the sample exposure period in Figures 2 and 3. Both weight gains and decreases are shown by the result fluctuations. The weight gain could be due to adherent corrosion products developing on the sample surfaces. As a result, the area of the substrate exposed to the corrosives may momentarily decrease. On the other hand, the weight loss might result from the flaws in the films disintegrating over a few days and progressively removing reinforcements.

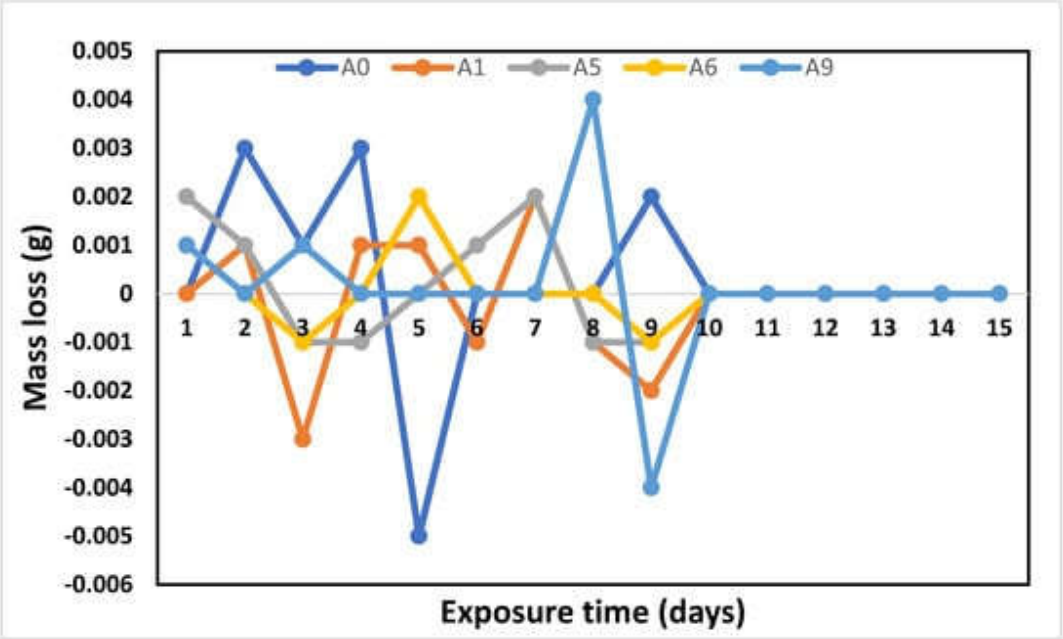

Figure 2: Mass changes of specimens against the time of exposure in 3.5 wt.% NaCl solution.

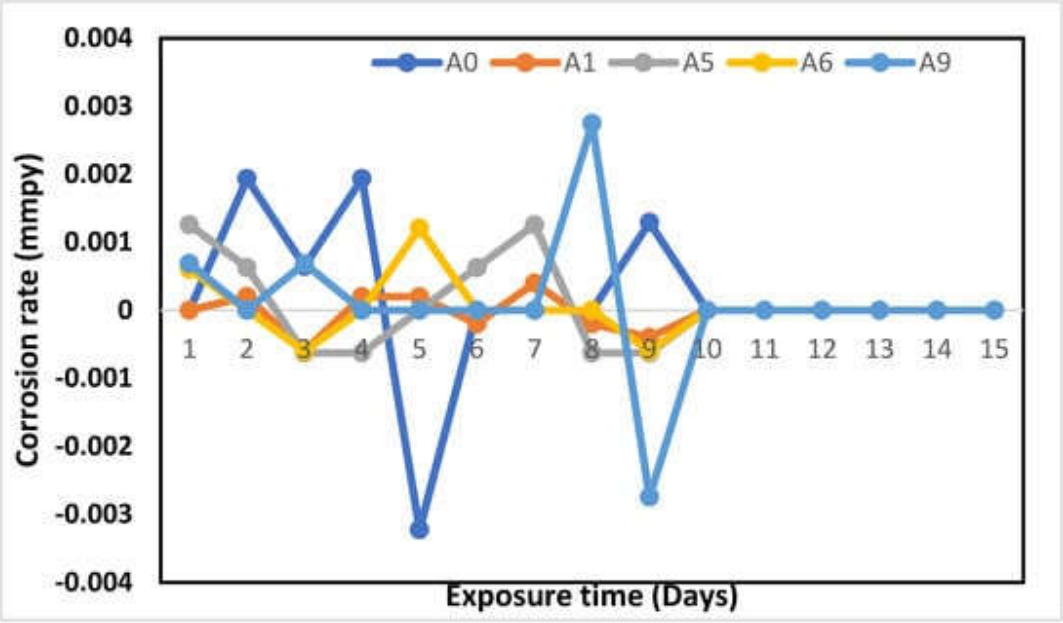

Figure 3: Corrosion rate of specimens versus the time of exposure in 3.5 wt.% NaCl solution.

The 3.5 weight percent NaCl solution has a mass loss of 0.04 grams. The composites may be appropriate for use in salty or marine settings with additional protection since they are almost stable and have some resistance to general corrosion in 3.5 weight percent NaCl. Comparable outcomes were found in this work and the study of Alaneme and Bodunrin [36], in which an alumina-reinforced Al5052 matrix was submerged in 3.5 weight percent NaCl. Because

the degree of corrosion rate was less than 0.1 mmpy, the reinforcement addition had a somewhat different impact on the corrosion behaviour than the unreinforced matrix. No matter what proportion of MoS_2 and Al_2O_3 are present in the composites, the corrosion behaviour remains constant. Nonetheless, monolithic (Al_2O_3 or GSA) reinforced samples demonstrated superior corrosion resistance compared to hybrid (Al_2O_3 and GSA) reinforced samples and unreinforced samples, according to research by Alaneme et al. [37]. The materials could be appropriate for usage in marine conditions based on the mass gain seen during the samples' gravimetric measurements. Because of the silica in MoS_2, the Al_2O_3 and Al interfacial interaction prevents the development of the Al_4C_3 phase, increasing the matrix's susceptibility to corrosion [37]. This is due to the fact that aluminum is not melted in silica crucibles. Al_2O_3 and Al do not react, however it is conceivable for intermetallic phases to develop that act as corrosion-initiation sites. Furthermore, the Al-Al_2O_3 composite is predicated on the reaction's absence.

Figure 4a, b show the obtained surface of the samples after exposure to NaCl solution for 15 days compared with the sample not immersed in the solution (Figure 4c). The corrosion behaviours of all the specimens are similar, with surges in the positive and negative directions reminiscent of observations made during potential measurements. Such surges infer some crack and heal events occurring at the bases of all the pits. The corrosion behaviors among all specimens are similar, with surges in the positive and negative directions reminiscent of observations made during potential measurements.

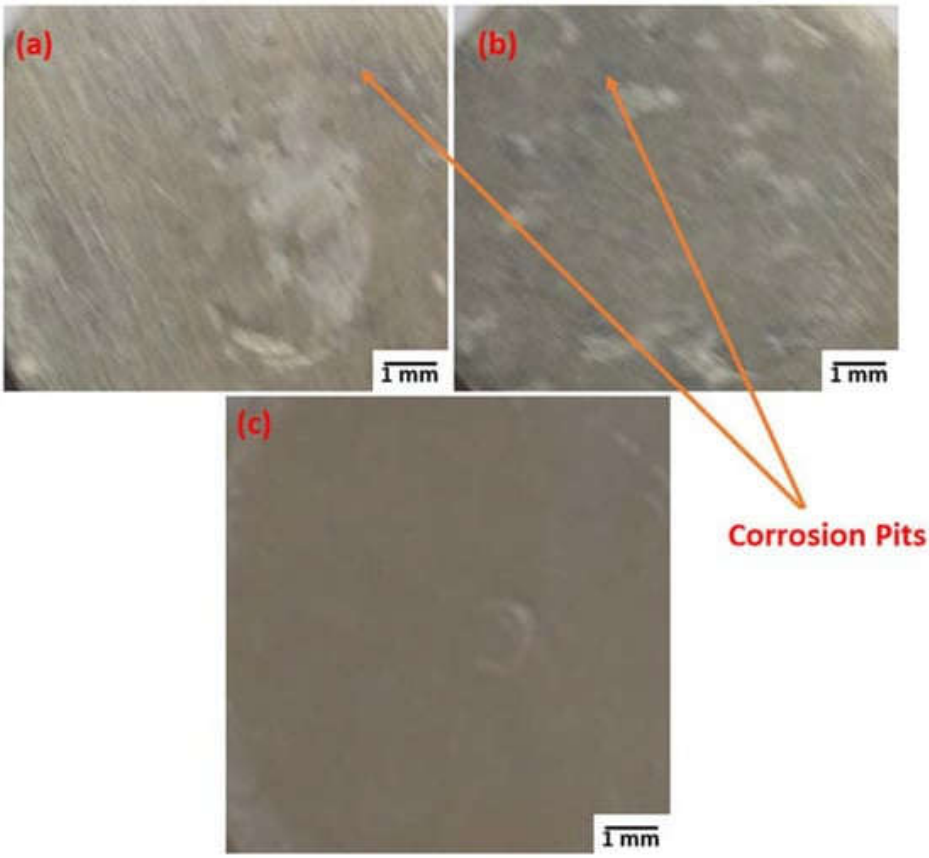

Figure 4: Corroded samples of (a) A9 and (b) A1 after immersion within the NaCl solution for 15 days (c) uncorroded sample.

The 3.5 wt.% NaCl solution (pH = 7.4) had very little pitting corrosion on the composites, though the pH level could be to blame for these findings. Four (4) steps of pitting corrosion are initiated by Cl ions. The hydrolysis within the corrosion product is invariably combined with metal oxidation within the corroding pits mechanism, producing localized acidity. The substantial separation of the cathodic half-reaction and the anodic half-reaction helps to maintain this localized acidity. The electrolyte gradually becomes more acidic as a result of insufficient oxygen penetration. Anion electrons migrate toward the created pit due to the acidity. The side products created during the corrosion process frequently fill the pits on the surface of metal.

The cathode is the surrounding surface that has been passivated, whereas anodic processes start on the metal surface that is exposed to the electrolyte. As a result, the particles from the second phase, the reinforcing inclusions, show up on the metal surface. As local anodes, the particles that precipitate along grain boundaries may cause localized galvanic corrosion and the emergence of early pits. Localized strains that manifest as dislocations on the surface have the potential to become anodes and start pits. For example, when exposed to a sodium chloride solution high in oxygen, the metal surface functions as a cathode and the pits that form as anodes. The electrolyte's chloride anions are eventually drawn to the excess positive charge created by the metal cations being produced in the pit. The ensuing molecules of the metal chloride now react with the water in the environment producing metal hydroxide and hydrochloric acid, further speeding up the corrosion rate.

Electrochemical Measurement among the specimens

Corrosion Behaviour in 3.5 wt.% NaCl Solution Using PDP

The potentiodynamic polarization curves of the composites exposed to 3.5% wt. NaCl solution for 24 and 72 h are shown in Figure 5a,b, respectively. The E_{corr} obtained is −0.22 V, which is nobler than those of reinforced specimens which are −0.761 V for A1, −0.885 V for A5, −0.863 V for A6, and −0.899 V for A9. The behaviors of the samples in NaCl indicated their susceptibility to corrosion attacks. This is an affirmation of what was observed during the gravimetric experiment. In 3.5% NaCl, the E_{corr} obtained was −220.62 mV. Furthermore, the corrosion current and potential shown in Figure 5a for the reinforced specimens were relatively low, with I_{corr} between 5.45 and 40.87 μA/cm² and E_{corr} between −220.62 and −899.48 mV. This phenomenon may be due to chloride attack at the aluminum–reinforcement interface.

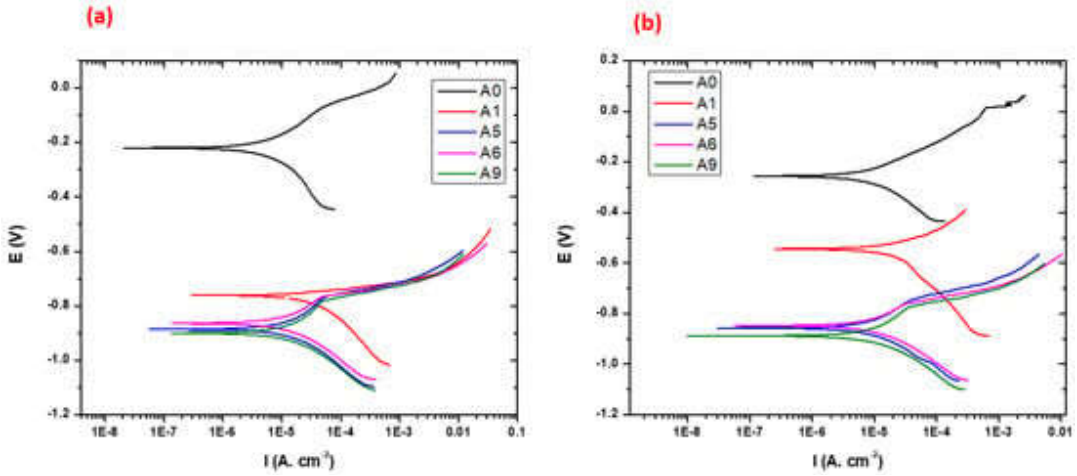

Figure 5: Polarization curves for the composites in 3.5% wt. NaCl solution at (a) 24 and (b) 72 h.

Table 3:

Sample Number	Composition
A1	Al 8088
A5	Al8088/TiO2 2%wt/ SiC 8%wt
A6	Al8088/TiO2 4%wt/ SiC 2%wt
A9	Al8088/TiO2 8%wt / SiC 2%wt

Table 3 shows I_{corr} and E_{corr} values for Samples A0, A1, A5, A6, and A9. At 24 h immersion in NaCl solution, it can be observed that sample A0 had the lowest I_{corr} value (5.45 μA/cm²), while at 72 h immersion time in NaCl solution, sample A5 gave the lowest I_{corr} value (6.809 μA/cm²). A low I_{corr} value indicates a low corrosion rate in NaCl solution. The unreinforced alloy showed an increase in I_{corr} values from when it was immersed in NaCl solution at 24 (5.45 μA/cm²) to 72 h (7.373 μA/cm²). This implies expectedly that the corrosion rate of the unreinforced alloy increased with exposure time in NaCl. The I_{corr} values of other samples immersed in NaCl solution increased at 72 h of exposure. However, the rate of increase in I_{corr} for the composites was lower than for the unreinforced alloy, and as discussed earlier, this is related to the potential pitting passivation window, which varies with exposure regimes, $\Delta E = (E_{pp} - E_{corr}) \geq 100$ mV. The summary of the E_{corr} and I_{corr} values of the samples is shown in Table 3.

Figure 5a,b reveal that irrespective of the exposure periods of the sample in the NaCl environment, the unreinforced sample A0 showed higher corrosion resistance than other samples. In addition, the sample reinforced with 2% TiO2 (sample A1) showed better corrosion resistance than samples A5, A6, and A9. The high corrosion resistance of sample A1 to other reinforced samples is due to the small amount of TiO2 reinforcement introduced into the matrix. Sample A6 with 2% SiC inclusion in its matrix showed better corrosion resistance compared to samples A5 and A9. However, the obtained value is far lower than the value achieved in sample A1. The presence of some metallic oxides in the SiC included in the matrix is a point of initiation of corrosion attacks in the NaCl environment. However, the hybrid reinforced composites of sample A5 (2% TiO2 and 8% SiC) and sample A9 (2% SiC and 8% TiO2) showed the least corrosion resistance in the subjected environment. This implied that 10% of the hybrid reinforced replacement in the Al matrix served as very strong active sites for pitting initiation.

EIS Spectra of the Samples

Figures 6 and 7 display the Bode plots of the samples that were submerged in a 3.5% NaCl solution for 24 and 72 hours, respectively. The samples' comparable patterns were visible in the impedance modulus against frequency Bode profile. The sample A0, which is unreinforced, has the highest impedance (Figure 6a). The reinforced composites could not quickly provide a protective film layer in the corrosive media like the unreinforced sample at 24 h immersion time. However, other samples showed better impedance modulus at 72 h immersion time in NaCl solution. It can be observed from Figure 7a that there was a steady rate of impedance modulus of the reinforced alloy in the NaCl solution with respect to the frequency values. This implied that the unreinforced sample may have shown better corrosion resistance, unlike the samples with reinforcement inclusions.

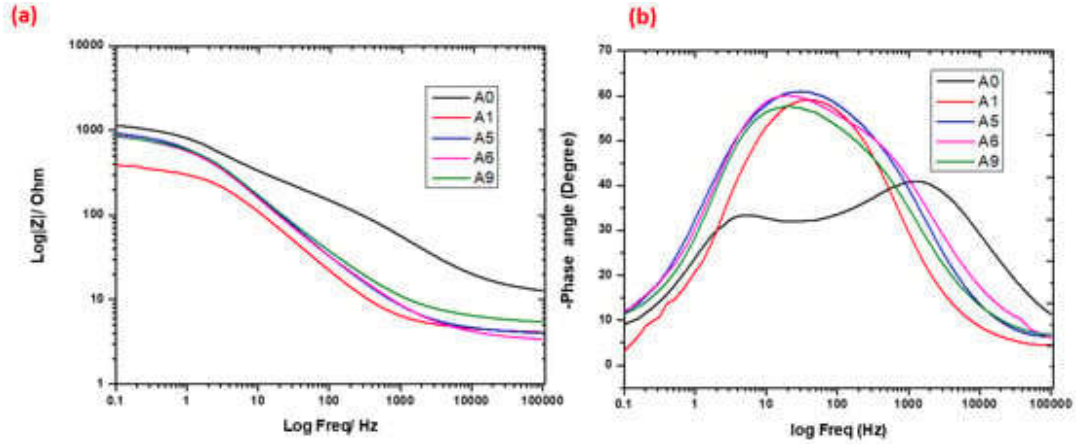

Figure 6: (a) Bode profiles, (b) Bode phase profiles of samples in 3.5% NaCl for 24 h.

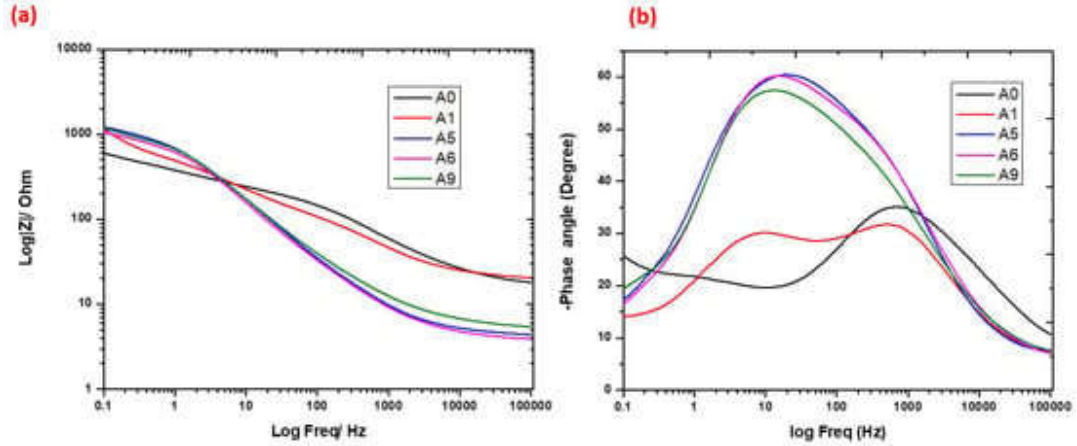

Figure 7: (a) Bode profiles, (b) Bode phase profiles of samples in 3.5% NaCl for 72 h.

The thin oxide layer that forms on the surfaces of the samples controls their corrosion resistance. This might have slowed down electrochemical reactions on the surfaces of the samples and limited ionic and electronic conductivity [38]. For the samples immersed in the NaCl solution (Table 4), it can be observed that samples A1, A5, A6, and A9 showed increased R_{ct} values in the 3.5% NaCl solution from 24 to 72 h immersion time. The R_{ct} values at 24 h immersion time for A1, A5, A6, and A9 were 382.6, 995.3, 880.4, and 903.1 $\Omega \cdot cm^2$ and increased to 979.7, 1080, 952.5, and 1040 $\Omega \cdot cm^2$ at 72 h immersion time, respectively. The increase in the R_{ct} values can be attributed to the decrease in the oxygen content present in the experimental setup as well as the quick formation of flawed oxide layers of corrosion products on the surface of the samples, which could impede further action of the solutions on the samples. The passive film resistance R_f values showed an initial decrease for sample A0 from 236 to 66.37 $\Omega \cdot cm^2$, while samples A1, A5, and A6 revealed increased R_f values at 24 to 72 h immersion time in 3.5% NaCl solution.

CONCLUSIONS

The influence of TiO2 and SiC reinforcements in Al8088 was preliminarily studied. The gravimetric analysis showed the presence of corrosion product formation with minimal pits. The corrosion mechanism of the samples immersed in NaCl solution was general and pitting corrosion. The composites displayed similar electrochemical behaviors in the 3.5% NaCl solution. Sample A0 (unreinforced alloy) initially exhibited greater corrosion resistance than the reinforced samples, but over time, this resistance waned. The inclusion of reinforcements or additives in the Al8088 matrix served as active sites for the start of corrosion. Stress raisers that are prone to pitting corrosion initiation sites are the result of the different chemical properties of the reinforcement inclusions in Al8088, which are likely to form discontinuous/flawed oxide layers wherever they intersect surfaces of the composites. In conclusion, the advanced protection in application areas will enable the use of the composites in areas less vulnerable to corrosion attack.

REFERENCES

1. Zakaria, H. M. (2014). Microstructural and corrosion behavior of Al/SiC metal matrix composites. Ain Shams Engineering Journal, 5(3), 831-838.
2. Peter P, I., & Adekunle A, A. (2020). A review of ceramic/bio-based hybrid reinforced aluminium matrix composites. *Cogent Engineering*, *7*(1), 1727167.
3. Ikubanni, P. P., Oki, M., Adeleke, A. A., Adediran, A. A., Agboola, O. O., Babayeju, O., ... & Omiogbemi, I. M. B. (2021). Tribological and physical properties of hybrid reinforced aluminium matrix composites. *Materials Today: Proceedings*, *46*, 5909-5913.
4. Omoniyi, P.O.; Akinlabi, E.T.; Mahamood, R.M.; Jen, T.C. Corrosion Resistance of Heat Treated Ti6Al4V in NaCl. *Chem. Data Collect.* **2021**, *36*, 100780.
5. Alaneme, K. K., Fajemisin, A. V., & Maledi, N. B. (2019). Development of aluminium-based composites reinforced with steel and graphite particles: structural, mechanical and wear characterization. Journal of Materials Research and Technology, 8(1), 670-682.
6. Haridass, R.; Vishnu, N.; Abinesh, A.; Manoj, K.N. (2018). Determination of corrosion behaviour of Al8088-TiO2-RHA meta matrix composites. *Int. J. Pure Appl. Math. 118*, 907–915.
7. Orhadahwe, T. A., Ajide, O. O., Adeleke, A. A., & Ikubanni, P. P. (2020). A review on primary synthesis and secondary treatment of aluminium matrix composites. *Arab Journal of Basic and Applied Sciences*, *27*(1), 389-405.
8. Ikubanni, P. P., Oki, M., Adeleke, A. A., & Agboola, O. O. (2021). Optimization of the tribological properties of hybrid reinforced aluminium matrix composites using Taguchi and Grey's relational analysis. *Scientific African*, *12*, e00839.
9. Nanjan, S., & Murali, J. G. (2020). Analysing the mechanical properties and corrosion phenomenon of reinforced metal matrix composite. Materials Research, 23(2), e20190681.
10. Ikubanni, P.P.; Oki, M.; Adeleke, A.A.; Omoniyi, P.O. (2021). Synthesis, phyTiO2o—Mechanical and microstructural characterization of Al8088/TiO2/SIC hybrid reinforced composites. *Sci. Rep. 11*, 14845.
11. Bodunrin, M.O.; Alaneme, K.K.; Chown, L.H. (2015). Aluminium matrix hybrid composites: A review of reinforcement philosophies; Mechanical, corrosion and tribological characteristics. *J. Mater. Res. Technol. 4*, 434–445.
12. Aigbodion, V. S., & Ezema, I. C. (2020). Multifunctional A356 alloy/PKSAnp composites: Microstructure and mechanical properties. Defence Technology, 16(3), 731-736.
13. Alaneme, K.K.; Oganbule, C.A.; Adewale, A. (2020). Circumferential notch test based fracture toughness investigation of Al-Mg-Si Alloy composites reinforced with alumina and quarry dust. *J. Chem. Technol. Metall. 55*, 469–478.
14. Edoziuno, F. O., Adediran, A. A., Odoni, B. U., Utu, O. G., & Olayanju, A. (2021). Physico-chemical and morphological

evaluation of palm kernel shell particulate reinforced aluminium matrix composites. *Materials Today: Proceedings*, *38*, 652-657.

15. Imran, M., & Khan, A. A. (2019). Characterization of Al-7075 metal matrix composites: a review. Journal of Materials Research and Technology, 8(3), 3347-3356.
16. Singh, G., & Goyal, S. (2018). Microstructure and mechanical behavior of AA6082-T6/SiC/B4C-based aluminum hybrid composites. Particulate Science and Technology, 36(2), 154-161.
17. Fatile, O. B., Akinruli, J. I., & Amori, A. A. (2014). Microstructure and mechanical behaviour of stir-cast Al-Mg-Sl alloy matrix hybrid composite reinforced with corn cob ash and silicon carbide. International Journal of Engineering and Technology Innovation, 4(4), 251-259.
18. Mavhungu, S. T., Akinlabi, E. T., Onitiri, M. A., & Varachia, F. M. (2017). Aluminum matrix composites for industrial use: advances and trends. Procedia Manufacturing, 7, 178-182.
19. Omoniyi, P.; Adekunle, A.; Ibitoye, S.; Olorunpomi, O.; Abolusoro, O. (2021). Mechanical and microstructural evaluation of aluminium matrix composite reinforced with wood particles. *J. King Saud Univ. Eng. Sci. 34*, 445–450.
20. Ikubanni, P.; Oki, M.; Adeleke, A.; Adesina, O.; Omoniyi, P. (2021). PhyTiO2o-Tribological Characteristics and Wear Mechanism of Hybrid Reinforced Al8088 Matrix Composites. *Acta Metall. Slovaca 27*, 172–179
21. Ikubanni, P.; Oki, M.; Adeleke, A.; Omoniyi, P.; Ajisegiri, E.; Akinlabi, E. (2022). PhyTiO2o-Mechanical Properties and Microstructure Responses of Hybrid Reinforced Al8088 Composites to SiC/TiO2 Inclusion. *Acta Metall. Slovaca***.** *28*, 25–32.
22. Gowda, H., & Prasad, P. R. (2016). Evaluation of mechanical properties of A356 alloy based hybrid composite at different aging conditions. Int J Sci Res Publ, 6(8).
23. Ononiwu, N.; Ozoegwu, C.; Madushele, N.; Akinribide, O.J. (2022). Mechanical Properties Tribology and Electrochemical Studies of Al/Fly Ash/Eggshell Aluminium Matrix Composite. *Biointerface Res. Appl. Chem. 12*, 4900–4919.
24. Omoniyi, P., Abolusoro, O., Olorunpomi, O., Ajiboye, T., Adewuyi, O., Aransiola, O., & Akinlabi, E. (2022). Corrosion properties of aluminum alloy reinforced with wood particles. Journal of Composites Science, 6(7), 189.
25. Alaneme, K. K., Ekperusi, J. O., & Oke, S. R. (2018). Corrosion behaviour of thermal cycled aluminium hybrid composites reinforced with rice husk ash and silicon carbide. *Journal of King Saud University-Engineering Sciences*, *30*(4), 391-397.
26. Prasad, D. S., Shoba, C., & Ramanaiah, N. (2014). Investigations on mechanical properties of aluminum hybrid composites. Journal of materials research and technology, 3(1), 79-85.
27. *Prasad, D. S., Shoba, C., & Ramanaiah, N. (2014). Investigations on mechanical properties of aluminum hybrid composites. Journal of materials research and technology, 3(1), 79-85.*
28. *Astm, I. (2016). ASTM E8/E8M-16a: standard test methods for tension testing of metallic materials. West Conshohocken, PA, USA: ASTM International.*
29. ASTM Committee G-1 on Corrosion of Metals. (2004). *Standard practice for laboratory immersion corrosion testing of metals*. ASTM International.
30. *ASTM G102-89*; Standard Practice for from Electrochemical Measurements 1. ASTM International: West Conshohocken, PA, USA, 2014; Volume 89, pp. 1–7.
31. Kanth, U. R., Rao, P. S., & Krishna, M. G. (2019). Mechanical behaviour of fly ash/SiC particles reinforced Al-Zn alloy-based metal matrix composites fabricated by stir casting method. Journal of Materials Research and Technology, 8(1), 737-744.
32. Alaneme, K. K., & Sanusi, K. O. (2015). Microstructural characteristics, mechanical and wear behaviour of aluminium matrix hybrid composites reinforced with alumina, rice husk ash and graphite. Engineering Science and Technology, an International Journal, 18(3), 416-422.
33. Sarada, B. N., Murthy, P. S., & Ugrasen, G. (2015). Hardness and wear characteristics

of hybrid aluminium metal matrix composites produced by stir casting technique. Materials Today: Proceedings, 2(4-5), 2878-2885.

34. Aigbodion, V.S. (2019). Bean pod ash nanoparticles a promising reinforcement for aluminium matrix bio composites. *J. Mater. Res. Technol.*, *8*, 6011–6020.
35. Anestiev, L., Lazarova, R., Petrov, P., Dyakova, V., & Stanev, L. (2021). On the strengthening and the strength reducing mechanisms at aluminium matrix composites reinforced with nano-sized TiCN particulates. Philosophical Magazine, 101(2), 129-153.
36. Alaneme, K.K.; Bodunrin, M.O. (2011). Corrosion Behavior of Alumina Reinforced Aluminium (8088) Metal Matrix Composites. *J. Miner. Mater. Charact. Eng. 10*, 1153–1165.
37. Alaneme, K. K., Eze, H. I., & Bodunrin, M. O. (2015). Corrosion behaviour of groundnut shell ash and silicon carbide hybrid reinforced Al-Mg-Si alloy matrix composites in 3.5% NaCl and 0.3 MH 2SO4 solutions. *Leonardo Electronic Journal of Practices and Technologies*, *26*, 129-146.
38. Alaneme, K. K., Ademilua, B. O., & Bodunrin, M. O. (2013). Mechanical properties and corrosion behaviour of aluminium hybrid composites reinforced with silicon carbide and bamboo leaf ash. Tribology in Industry, 35(1), 25.

****